

Highly-Sensitive MEMS Micro-Fluxgate Magnetometer

Ziwei Wang¹, Ying Shen¹, Chong Lei, Jiazeng Wang, Shuxiang Zhao, Jiamin Chen²,
Zhaoqiang Chu, and Junqi Gao¹

Abstract—Fluxgate magnetometers have been widely applied in many fields, such as magnetic anomaly detection, e-compass, etc. In this work, a micro-fluxgate magnetometer based on the implementation of the MEMS technology is proposed. The core of the fluxgate was fabricated by using an amorphous Co-based magnetic material, which shows a good degree of linearity below 0.5 Oe. Moreover, a mixed-signal lock-in circuit was designed to drive and capture signals. Magnetic noise density of such a device was limited to the value of 500 pT/ $\sqrt{\text{Hz}}$ at 1 Hz, while the capability of sensing a DC magnetic field of 6 nT was demonstrated, which presents a good development prospect in the weak signal detection domain.

Index Terms—Micro-fluxgate, lock-in circuit, weak magnetic detection.

I. INTRODUCTION

THROUGH the behavior research of nearly 50 kinds of animals including birds, turtles and sharks, it was found that animals can navigate and locate by sensing the Earth's magnetic field, which excites a great interest of developing novel GPS based on geomagnetic field [1]–[3]. To date, several types of magnetometers can be found on the market, such as superconducting quantum interference device (SQUID), optically-pumped magnetometers, magnetoresistance (MR) sensors and so on, which play a key role in the magnetic field detection [4], [5].

Manuscript received 5 June 2022; revised 23 June 2022; accepted 23 June 2022. Date of publication 1 July 2022; date of current version 26 July 2022. This work was supported in part by the National Key Research and Development Program of China under Grant 2021YFB2011600, in part by the National Natural Science Foundation of China under Grant 62101151, in part by the Natural Science Foundation of Heilongjiang Province of China under Grant G3121054, in part by the Natural Science Foundation of Shandong Province under Grant ZR2021MF106, and in part by the National Major Scientific Instruments and Equipments Development Project of National Natural Science Foundation of China under Grant 42127807-03. The review of this letter was arranged by Editor H. Lee. (Corresponding author: Junqi Gao.)

Ziwei Wang, Ying Shen, Jiazeng Wang, Shuxiang Zhao, Zhaoqiang Chu, and Junqi Gao are with the Acoustic Science and Technology Laboratory, Harbin 150001, China, also with the Key Laboratory of Marine Information Acquisition and Security, Ministry of Industry and Information Technology, Harbin Engineering University, Harbin 150001, China, and also with the College of Underwater Acoustic Engineering, Harbin Engineering University, Harbin 150001, China (e-mail: gaojunqi@hrbeu.edu.cn).

Chong Lei is with the Key Laboratory of Thin Film and Microfabrication (Ministry of Education), Department of Micro-Nano Electronics, School of Electronic Information and Electrical Engineering, Shanghai Jiao Tong University, Shanghai 200240, China.

Jiamin Chen is with the State Key Laboratory of Transducer Technology, Aerospace Information Research Institute, Chinese Academy of Sciences, Beijing 100094, China.

Color versions of one or more figures in this letter are available at <https://doi.org/10.1109/LED.2022.3187447>.

Digital Object Identifier 10.1109/LED.2022.3187447

Although the conventional fluxgate sensors are widely used for several magnetic detection applications, they possess many problems, like large volume, high power consumption and high fabrication cost due to their structural characteristics [6]. The emergence of MEMS technology is anticipated to significantly assist in overcoming these limitations [7], [8].

Therefore, the design of MEMS fluxgate sensors and the optimization of the magnetic field detection capabilities have been widely reported in the literature [9]–[12]. More specifically, it has been demonstrated that the demagnetization effect, permeability and structural configuration play an important role in the total sensing performance [13]–[15]. In addition, temperature [4] and the peripheral electronic circuits [16] also affect the performance of the fluxgate sensor. A three-axis fluxgate sensor employs a special gimbaled construction that exhibits high stability and low noise, which is suitable for long-term geomagnetic vector field measurements [17]. By using the MEMS technology, different core materials and core structures have been proposed by combining integration technology [15], [18], melt spinning [6] and other technologies [19]. Beyond that, the sensitivity and the linear range of the fluxgate sensor can be also improved by optimizing the lock-in circuit [20]–[23].

Although many breakthroughs have been reported, the micro-fluxgate magnetometers have not been well developed due to limitations of the lock-in circuit. Under this direction, in this work, a micro-fluxgate magnetometer is proposed in conjunction with a mixed-signal lock-in circuit, which shows great detection properties. The development of such type of portable magnetometer is quite promising for weak field detection applications.

II. MICRO-FLUXGATE MAGNETOMETER DESIGN

A micro-fluxgate magnetometer was proposed to contain a micro-fluxgate and a custom lock-in circuit. The fluxgate was fabricated by a standard MEMS processing [24]. As far as the lock-in circuit is concerned, it is a mixed-signal circuit containing a digital signal generator and an analog demodulator.

A. Micro-Fluxgate Design

The active core of the MEMS fluxgate was made by using an amorphous Co-based soft magnetic material (VITROVAC 6025Z). Fig. 1 shows the fabrication processing including thick photoresist-based UV lithography, sputtering, electroplating of Cu film, dry and wet etching of excess materials, etc. More details can be found in our previous work [18].

As is illustrated in Fig. 2 (a), this MEMS fluxgate sensor contains a rectangular magnetic core, which is wrapped by two pairs of driving coils to generate a high-frequency driving magnetic field. In addition, a pick-up coil is integrated at the

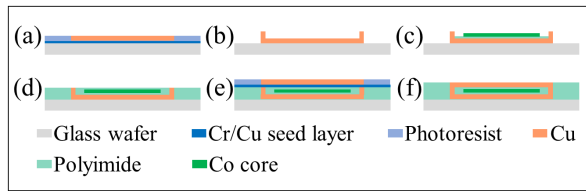


Fig. 1. Schematic illustration of the fabrication steps of the MEMS-based fluxgate sensor. (a) Electroplating of the bottom coils; (b) electroplating of the vias; (c) pasting of core; (d) polishing of polyimide; (e) electroplating of the top coils and electrodes; and (f) polishing of polyimide.

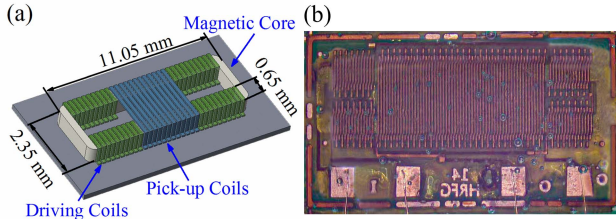


Fig. 2. (a) Schematic diagram; and (b) photograph of MEMS fluxgate sensor.

center of the magnetic core to collect the signals induced by variations of magnetic flux.

Moreover, the rectangular magnetic core was 11.05 mm \times 2.35 mm in size and had a thickness of 15 μ m to obtain better performance. The long side width of the rectangular core was 650 μ m. In addition, the numbers of turns for the driving coils and pick-up coils were 62 and 59, respectively, whereas the packaging dimension of the micro-fluxgate was around 12 mm \times 7 mm, as is shown in Fig. 2 (b).

The property of the micro-fluxgate in response to the external magnetic field was systematically characterized. During the measurements, the device and a solenoid coil were placed inside a magnetic shielding chamber to block the external noise. The solenoid coil was powered by a current source to apply a DC magnetic field along the sensitive axis of the micro-fluxgate.

According to our previous work [18], optimized driving frequency exists by considering the sensitivity, the noise and the power consumption of a fluxgate system. In the proposed design, the sensitivity of the micro-fluxgate can be enhanced by initially increasing the driving frequency. However, the response of the sensor is not consistent as the driving frequency exceeds the value of 400 kHz, which is caused by the manifestation of the nonlinear skin effect. Meanwhile, the noise level was also improved under this condition. Thus, a functional generator was used to excite the driving coils at a frequency value of 400 kHz with an amplitude of 60 mA. Moreover, only the second harmonic signal was induced by pick-up coils, which is directly related to the amplitude of the external magnetic field based on the working principle of the fluxgate. Therefore, a pre-amplifier (SR560) was used to amplify the second harmonic signal by setting up a band pass filter around the value of 800 kHz. The amplified signal was then monitored by an oscilloscope. The measured result is depicted in Fig. 3, and the M-H curve of the Co core was added as an insert graph.

From the extracted outcomes, it can be argued that the micro-fluxgate shows a linear response to the external magnetic field at the range of ± 1 Oe, which is considered satisfactory for the majority of geomantic field detection applications.

B. Readout Circuit Design

The overall architecture of the specially designed lock-in circuit is shown in Fig. 4. One of the most important parts

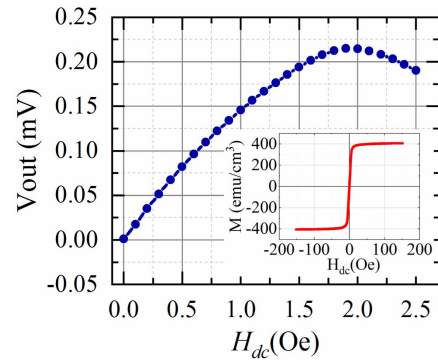


Fig. 3. Distribution of the output signal of the micro-fluxgate as a function of the DC magnetic field. The inset graph depicts the M-H curve of the core.

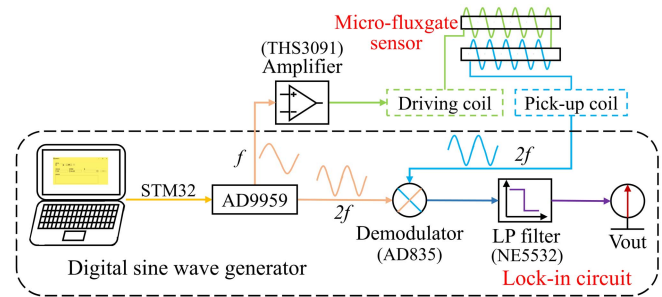


Fig. 4. Depiction of the functional block of the lock-in circuit.

of the proposed circuit is the high-frequency signal generator. In this design, a digital circuit module based on AD 9959 was also implemented. Benefitting from this signal generator, the key parameters of the driving signal and reference signal including the frequency, as well as the amplitude and phase, can be continuously tuned by a program, which shows the great advantage of the developed architecture over the analog lock-in circuit with fixing electronic parameters. On the other hand, the proposed circuit is more complicated and the power consumption is relatively higher. However, the latter can be further optimized. Based on the above-mentioned measurements, the amplitude of the driving signal was set at the value of 1 V with a frequency of 400 kHz, while the frequency of the reference signal was set at 800 kHz.

On the other hand, an analog demodulator based on AD835 was utilized. By using this module, the induced signal from the micro-fluxgate and the reference signal was multiplied. The process can be expressed as follows:

$$\begin{aligned}
 V_{output} &= V_{micro-fluxgate} \times V_{ref} \\
 &= AB \sin 2\omega_0 t \cdot \sin (2\omega_0 t + \Delta\phi) \\
 &= \frac{AB}{2} [\cos \Delta\phi - \cos (4\omega_0 t + \Delta\phi)] \quad (1)
 \end{aligned}$$

where V_{output} represents the output signal through demodulation process, A and B denote the amplitudes of the reference signal and induced signal of the micro-fluxgate, respectively, ω_0 is the driving frequency, and $\Delta\phi$ is the phase difference between these two signals.

Clearly, the output signal is composed of a DC signal and an AC signal, whereas is comprised of the following component: $4\omega_0$. Next, a low pass filter was designed to obtain the DC component by rejecting the high-frequency signal.

In this case, the relationship between the measured DC magnetic field and the DC output is $V_{out} = S \times H_{dc}$, where S stands for the sensitivity in the unit of V/Oe.

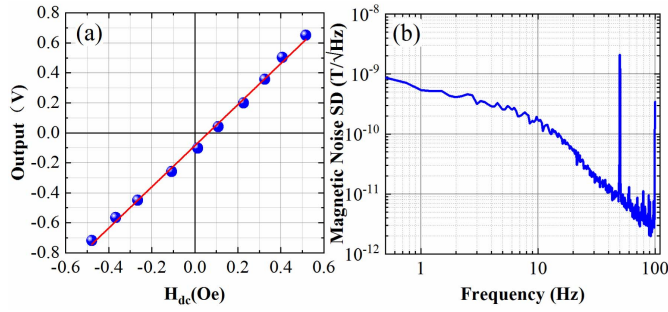


Fig. 5. (a) Output signal of the micro-fluxgate sensor as a function of the DC magnetic field; and (b) equivalent magnetic noise SD.

III. RESULTS AND DISCUSSIONS

A. Sensitivity and Noise

Firstly, the sensitivity of the micro-fluxgate magnetometer was characterized. During the test, the device was placed in the center of a Helmholtz coil, which was powered by a current source to generate a DC magnetic field along the sensitive axis of the sensor. Because the coils of the sensor were quite small and the distance between the sensor and Helmholtz coil was large enough, the mutual inductance coupling effect can be ignored. The amplitude of the magnetic field was monitored by using a gauss meter. Finally, the output of the sensor was monitored by a digital multimeter. The DC output voltage as a function of the magnetic field is displayed in Fig. 5 (a), where the scattering points represent the measured data. A linear fitting was also performed, which is indicated by the solid red line. As can be ascertained, a desirable linearity within the range of -0.5 to 0.5 Oe was attained by the proposed fluxgate sensing element. Clearly, the value of the sensitivity of the micro-fluxgate magnetometer was determined to be 1.27 V/Oe.

Besides the sensitivity, another important parameter for practical applications is the intrinsic noise, which was also measured for the introduced micro-fluxgate magnetometer. To eliminate the external magnetic interference, the magnetometer was placed inside the magnetically shielding chamber. Moreover, the output of the unit was connected to a dynamic signal analyzer (SR 785) to obtain the power spectral density.

By using SR 785, the voltage noise spectral density (SD) can be directly obtained. To get the equivalent magnetic noise SD, the following equation was used to convert the unit from $V/\sqrt{\text{Hz}}$ to $T/\sqrt{\text{Hz}}$:

$$M_{SD}(T/\sqrt{\text{Hz}}) = \frac{V_{SD}(V/\sqrt{\text{Hz}})}{S(V/\text{Oe})} \times 10^{-4} \quad (2)$$

As can be observed from Fig. 5 (b), the noise at the low-frequency range was dominated by $1/f$ noise, as was expected. Additionally, the noise was attenuated sharply above the value of 10 Hz due to the low-pass filter. More specifically, the magnetic noise SD at 1 Hz was 500 pT/ $\sqrt{\text{Hz}}$.

B. Resolution

The DC magnetic field resolution of the micro-fluxgate magnetometer was also measured. During the test, a small number of H-coils and the device were placed inside the chamber. A DC power source was used to drive the H-coils for generating a tiny magnetic field. By controlling the source, a magnetic field step with an amplitude of 6 nT was applied to the sensor. By considering the geometry of the magnetic core, its demagnetization factor was quite close to 0 . Thus,

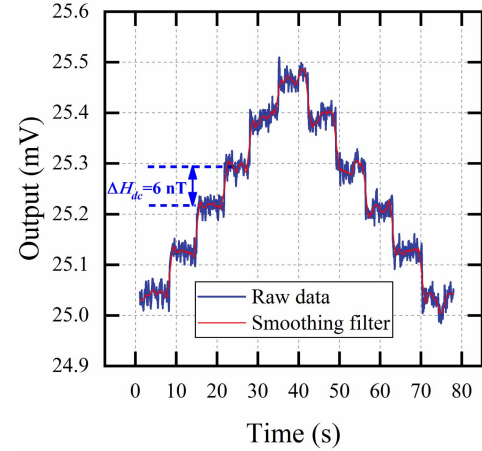


Fig. 6. Resolution of the micro-fluxgate magnetometer under the application of small DC magnetic field variations.

TABLE I
PERFORMANCE COMPARISON OF THE DIFFERENT SENSORS

Technology	Size (mm ²)	Noise SD (pT/ $\sqrt{\text{Hz}}$)	Resolution (nT)	Ref
Micro-fluxgate (closed core)	-	24000	-	[25]
ME (Metglas/polyvinylidene-fluoride)	-	-	8	[26]
Micro fluxgate sensor	4.65×5.04	2480	-	[27]
ME (Metglas/FeNi/PZT)	25×6	-	7	[28]
Co-based amorphous ribbon fluxgate sensor	30×65	790	-	[29]
TMR9003	6×5	750	-	Data sheet
Hall sensor	0.7×2.1	-	1.18×10^5	[30]
MEMS fluxgate sensor	10×2.7	1150	-	[15]
ME (Metglas/PZT)	-	128	1	[31]
Meander-Core orthogonal fluxgate	-	111.6	-	[13]
This work	12×7	500	6	-

almost all of the external magnetic field was applied to the sensor. As was expected, an output voltage step function of the magnetometer could be detected, as is shown in Fig. 6. This result clearly demonstrates that the designed micro-fluxgate has an excellent detection ability of a 6 nT DC magnetic field. Moreover, no hysteresis effects and good repeatability were also captured by the sensor.

The performance of different types of MEMS-based magnetic sensors is summarized in Table I. Interestingly, the proposed micro-fluxgate magnetometer presents an excellent capability of detecting small DC magnetic fields compared to the majority of the reported sensing elements. However, the noise SD of this fluxgate sensor needs to be eliminated to further improve its resolution.

IV. CONCLUSION

In this work, a compact fluxgate magnetometer was proposed, which consisted of a micro-fluxgate and a lock-in circuit. The sensitivity and the magnetic noise SD of the proposed sensor were 1.27 V/Oe and 500 pT/ $\sqrt{\text{Hz}}$ at 1 Hz, respectively. With regard to the detection accuracy, the proposed sensor has a high detection resolution of 6 nT, which stems from the high sensitivity and low noise. Thus, the development of a micro-fluxgate magnetometer by using MEMS technology offers unique perspectives in the field of weak magnetic detection.

REFERENCES

- [1] P. J. Hore, K. B. Henbest, F. Cintolesi, I. Kuprov, C. T. Rodgers, P. A. Liddell, D. Gust, C. R. Timmel, and P. J. Hore, "Chemical compass model of avian magnetoreception," *Nature*, vol. 453, pp. 387–390, May 2008, doi: [10.1038/nature06834](https://doi.org/10.1038/nature06834).
- [2] K. J. Lohmann, S. D. Cain, S. A. Dodge, and C. M. F. Lohmann, "Regional magnetic fields as navigational markers for sea turtles," *Science*, vol. 294, no. 5541, pp. 364–366, Oct. 2001, doi: [10.1126/science.1064557](https://doi.org/10.1126/science.1064557).
- [3] C. G. Meyer, K. N. Holland, and Y. P. Papastamatiou, "Sharks can detect changes in the geomagnetic field," *J. Roy. Soc. Interface*, vol. 2, no. 2, pp. 129–130, Mar. 2005, doi: [10.1098/rsif.2004.0021](https://doi.org/10.1098/rsif.2004.0021).
- [4] U. Topal, P. Svec, H. Can, F. Celik, C. Birlıkseven, I. Skorvanek, F. Andrejka, B. Kunca, J. Marcin, P. Svec, I. Janotova, and A. Uygur, "Optimization of the temperature stability of fluxgate sensors for space applications," *IEEE Sensors J.*, vol. 21, no. 3, pp. 2749–2756, Feb. 2021, doi: [10.1109/JSEN.2020.3024547](https://doi.org/10.1109/JSEN.2020.3024547).
- [5] J. Lenz and A. S. Edelstein, "Magnetic sensors and their applications," *IEEE Sensors J.*, vol. 6, no. 3, pp. 631–649, Jun. 2006, doi: [10.1109/JSEN.2006.874493](https://doi.org/10.1109/JSEN.2006.874493).
- [6] L. Guo, C. Wang, S. Zhi, Z. Feng, C. Lei, and Y. Zhou, "Wide linearity range and highly sensitive MEMS-based micro-fluxgate sensor with double-layer magnetic core made of Fe–Co–B amorphous alloy," *Micro-machines*, vol. 8, no. 12, p. 352, Nov. 2017, doi: [10.3390/mi8120352](https://doi.org/10.3390/mi8120352).
- [7] R. Savarapu, A. Sohan, and P. Kollu, "Fabrication advancements in integrated fluxgate sensors: A mini review," *Adv. Eng. Mater.*, vol. 24, no. 4, Apr. 2022, Art. no. 2101040, doi: [10.1002/adem.202101040](https://doi.org/10.1002/adem.202101040).
- [8] J. Gao, J. Wang, Y. Shen, Z. Jiang, Y. Huang, and Q. Yu, "Equivalent magnetic noise analysis for a tunneling magnetoresistive magnetometer," *IEEE Electron Device Lett.*, vol. 41, no. 9, pp. 1400–1403, Sep. 2020, doi: [10.1109/LED.2020.3007950](https://doi.org/10.1109/LED.2020.3007950).
- [9] T. Charubin, M. Nowicki, and R. Szewczyk, "Investigation of high order harmonic for signal extraction in Matteucci effect based fluxgate magnetic sensors," in *Proc. Appl. Phys. Condens. MATTER (APCOM)*, Slovakia, Europe, 2019, Art. no. 020018, doi: [10.1063/1.5119471](https://doi.org/10.1063/1.5119471).
- [10] U. Topal, H. Can, O. M. Çelik, A. Narman, M. Kamiş, V. Çitak, D. Çakrak, H. Sözeri, and P. Svec, "Design of fluxgate sensors for different applications from geology to medicine," *J. Supercond. Novel Magnetism*, vol. 32, no. 4, pp. 839–844, Apr. 2019, doi: [10.1007/s10948-018-4781-x](https://doi.org/10.1007/s10948-018-4781-x).
- [11] S. L. Yang and R. Fan, "Flexible-substrate fluxgate current sensor based on MEMS technology," *Sensors Mater.*, vol. 32, no. 9, pp. 3083–3094, 2020, doi: [10.18494/SAM.2020.2737](https://doi.org/10.18494/SAM.2020.2737).
- [12] H. Lv and S. Liu, "Low power consumption design and fabrication of thin film core for micro fluxgate," *J. Nanosci. Nanotechnol.*, vol. 16, no. 3, pp. 2663–2667, Mar. 2016, doi: [10.1166/JNN.2016.10773](https://doi.org/10.1166/JNN.2016.10773).
- [13] S. Zhi, X. Sun, Q. Zhang, J. Chen, X. Zhang, H. Chen, and C. Lei, "Demagnetization effect in a meander-core orthogonal fluxgate sensor," *Micromachines*, vol. 12, no. 8, p. 937, Aug. 2021, doi: [10.3390/mi12080937](https://doi.org/10.3390/mi12080937).
- [14] Y. Liu, Z. Yang, T. Wang, X.-C. Sun, C. Lei, and Y. Zhou, "Improved performance of the micro planar double-axis fluxgate sensors with different magnetic core materials and structures," *Microsyst. Technol.*, vol. 22, no. 9, pp. 2341–2347, Sep. 2016, doi: [10.1007/s00542-015-2618-0](https://doi.org/10.1007/s00542-015-2618-0).
- [15] C. Lei, X.-C. Sun, and Y. Zhou, "Noise analysis and improvement of a micro-electro-mechanical-systems fluxgate sensor," *Measurement*, vol. 122, pp. 1–5, Jul. 2018, doi: [10.1016/j.measurement.2018.03.007](https://doi.org/10.1016/j.measurement.2018.03.007).
- [16] P. D. Dimitropoulos and J. N. Avaritsiotis, "A micro-fluxgate sensor based on the Matteucci effect of amorphous magnetic fibers," *Sens. Actuators A, Phys.*, vol. 94, no. 3, pp. 165–176, 2001, doi: [10.1016/S0924-4247\(01\)00706-3](https://doi.org/10.1016/S0924-4247(01)00706-3).
- [17] X. Wang, Y. Teng, X. Fan, C. Wang, Q. Wu, and J. Ma, "Design of a suspended high-stability fluxgate sensor," *Meas. Sci. Technol.*, vol. 32, no. 6, Jun. 2021, Art. no. 065101, doi: [10.1088/1361-6501/abd514](https://doi.org/10.1088/1361-6501/abd514).
- [18] C. Lei, Y. Liu, X.-C. Sun, T. Wang, Z. Yang, and Y. Zhou, "Improved performance of integrated solenoid fluxgate sensor chip using a bilayer Co-based ribbon core," *IEEE Sensors J.*, vol. 15, no. 9, pp. 5010–5014, Sep. 2015, doi: [10.1109/JSEN.2015.2432457](https://doi.org/10.1109/JSEN.2015.2432457).
- [19] P. Frydrych, R. Szewczyk, J. Salach, and K. Trzcinka, "Two-axis, miniature fluxgate sensors," *IEEE Trans. Magn.*, vol. 48, no. 4, pp. 1485–1488, Apr. 2012, doi: [10.1109/TMAG.2011.2173475](https://doi.org/10.1109/TMAG.2011.2173475).
- [20] M. Ayat, M. A. Karami, S. Mirzakuchaki, and A. Beheshti-Shirazi, "Design of multiple modulated frequency lock-in amplifier for tapping-mode atomic force microscopy systems," *IEEE Trans. Instrum. Meas.*, vol. 65, no. 10, pp. 2284–2292, Jul. 2016, doi: [10.1109/TIM.2016.2579438](https://doi.org/10.1109/TIM.2016.2579438).
- [21] M. Chandra, A. Sharma, A. Roy, A. Venkatesh, S. S. Kamble, J. K. Radhakrishnan, and U. K. Singh, "Implementation of digital lock-in and concentration measurement for wavelength modulation spectroscopy (WMS) based sensors using MATLAB," in *Proc. 3rd Int. Conf. Sens., Signal Process. Secur. (ICSSS)*, May 2017, pp. 350–356, doi: [10.1109/SSPS.2017.8071619](https://doi.org/10.1109/SSPS.2017.8071619).
- [22] C. Kolacinski and D. Obrebski, "Multichannel integrated lock-in amplifier for low noise measurements," in *Proc. MIXDES*, Bydgoszcz, Poland, Jun. 2017, pp. 290–295.
- [23] G. Macias-Bobadilla, J. Rodríguez-Reséndiz, G. Mota-Valtierra, G. Soto-Zarazúa, M. Méndez-Loyola, and M. Garduño-Aparicio, "Dual-phase lock-in amplifier based on FPGA for low-frequencies experiments," *Sensors*, vol. 16, no. 3, p. 379, Mar. 2016, doi: [10.3390/s16030379](https://doi.org/10.3390/s16030379).
- [24] C. Lei, Y. Liu, X.-C. Sun, T. Wang, Z. Yang, and Y. Zhou, "Improved performance of integrated solenoid fluxgate sensor chip using a bilayer Co-based ribbon core," *IEEE Sensors J.*, vol. 15, no. 9, pp. 5010–5014, Sep. 2015, doi: [10.1109/JSEN.2015.2432457](https://doi.org/10.1109/JSEN.2015.2432457).
- [25] P. Ripka, S. Kawahito, S. O. Choi, A. Típek, and M. Ishida, "Micro-fluxgate sensor with closed core," *Sens. Actuators A, Phys.*, vol. 91, nos. 1–2, pp. 65–69, 2001, doi: [10.1016/S0924-4247\(01\)00481-2](https://doi.org/10.1016/S0924-4247(01)00481-2).
- [26] J. Zhai, S. Dong, Z. Xing, J. Li, and D. Viehland, "Giant magnetoelectric effect in Metglas/polyvinylidene-fluoride laminates," *Appl. Phys. Lett.*, vol. 89, no. 8, Aug. 2006, Art. no. 083507, doi: [10.1063/1.2337996](https://doi.org/10.1063/1.2337996).
- [27] J. Lei, C. Lei, and Y. Zhou, "Analysis and comparison of the performance of MEMS fluxgate sensors with permalloy magnetic cores of different structures," *Measurement*, vol. 46, no. 1, pp. 710–715, Jan. 2013, doi: [10.1016/j.measurement.2012.09.009](https://doi.org/10.1016/j.measurement.2012.09.009).
- [28] J. G. Tao, Y. Y. Jia, H. Wu, and J. G. Yang, "Low-frequency nanotesla resolution of magnetic field detection in metglas/magnetostrictive/piezoelectric laminates," *Adv. Mater. Res.*, vols. 960–961, pp. 695–699, Jun. 2014, doi: [10.4028/www.scientific.net/AMR.960-961.695](https://doi.org/10.4028/www.scientific.net/AMR.960-961.695).
- [29] C. C. Lu, J. Huang, P. K. Chiu, S. L. Chiu, and J. T. Jeng, "High-sensitivity low-noise miniature fluxgate magnetometers using a flip chip conceptual design," *Sensors*, vol. 14, no. 8, pp. 13815–13829, Jul. 2014, doi: [10.3390/s140813815](https://doi.org/10.3390/s140813815).
- [30] M. Kachniarz, O. Petruk, M. Oszwaldowski, J. Salach, T. Ciuk, W. Strupiński, W. Winiarski, and K. Trzcinka, "Influence of protective layer on the functional properties of monolayer and bilayer graphene Hall-effect sensors," in *Proc. Adv. Intell. Syst. Comput.*, 2015, pp. 101–109, doi: [10.1007/978-3-319-15835-8_12](https://doi.org/10.1007/978-3-319-15835-8_12).
- [31] Y. Shen, D. Ma, and J. Gao, "A man-portable magnetoelectric DC magnetic sensor with extremely high sensitivity," *IEEE Electron Device Lett.*, vol. 39, no. 9, pp. 1417–1420, Sep. 2018, doi: [10.1109/LED.2018.2858280](https://doi.org/10.1109/LED.2018.2858280).